Geoderma 390 (2021) 114952

Contents lists available at ScienceDirect

Geoderma

journal homepage: www.elsevier.com/locate/geoderma

Integrative effects of increasing aridity and biotic cover on soil attributes and functioning in coastal dune ecosystems

María José Fernández-Alonso[a,*], Alexandra Rodríguez[a], Laura García-Velázquez[b], Everaldo Dos Santos[c], Luciana de Almeida[a], Angela Lafuente[d,e], Jun-Tao Wang[f,g], Brajesh Singh[f,g], David Fangueiro[h], Jorge Durán[a]

[a] *Centre for Functional Ecology, Department of Life Sciences, University of Coimbra, Calçada Martim de Freitas, 3000-456 Coimbra, Portugal*
[b] *Departamento de Sistemas Físicos, Químicos y Naturales, Universidad Pablo de Olavide, Crta. Utrera km 1, 41013 Sevilla, Spain*
[c] *Eixo de Recursos Naturais/Meio Ambiente, Campus Paranaguá-PR, Instituto Federal de Educação Ciência e Tecnologia do Paraná, CEP 83215-750 N° 453, Paranaguá, Brazil*
[d] *Departamento de Biología y Geología, Física y Química Inorgánica, Escuela Superior de Ciencias Experimentales y Tecnología, Universidad Rey Juan Carlos, Calle Tulipán s/n, 28933 Móstoles, Spain*
[e] *School of Forest Resources and Environmental Science, Michigan Technological University, Houghton, MI 49931, USA*
[f] *Hawkesbury Institute for the Environment, Western Sydney University, Penrith, NSW 2751, Australia*
[g] *Global Centre for Land-Based Innovation, Western Sydney University, Penrith, NSW 2751, Australia*
[h] *LEAF, Instituto Superior de Agronomia, Universidade de Lisboa, Tapada da Ajuda, 1349-017 Lisboa, Portugal*

A R T I C L E I N F O

Handling Editor: Naoise Nunan

Keywords:
Soil fertility
Greenhouse gas fluxes
Soil microbial community
Nutrient cycling
Spatial variability
Drylands

A B S T R A C T

Climate change-driven increases in aridity will lead to dryland expansion worldwide. In the Atlantic and Mediterranean biogeographic regions, coastal dunes are priority conservation areas highly sensitive to aridification where plants and biological soil crusts may play a key role maintaining ecosystem services. However, we still need further insights into the balance between the effects of increasing aridity and the influence of local vegetation on the soil attributes and functioning of these systems, particularly in transitional areas between humid and arid climatic zones. We sampled 24 dune systems distributed along a natural climate gradient including humid, dry-subhumid and arid environments in the Atlantic coastline of the Iberian Peninsula and investigated (i) how aridity drives the vegetation community structure, soil biotic and abiotic properties and functions in dune ecosystems at a regional scale; and (ii) to what extent soil attributes differ locally under diverse surface microsites (i.e. plants, biocrust and bare soil). Increasing aridity in coastal dunes decreased total biotic cover and favoured the formation of shrub-dominated patches. Vegetation shifts were accompanied by declines in soil microbial diversity, organic matter, nutrient contents and reduced rates of N mineralization. Soil bacterial communities were more sensitive to aridity than fungal communities. Microsites were essential regulators of soil attributes, and their effects were dependent on the degree of aridity. In drylands, shrub microsites were associated to higher soil organic C, microbial (bacterial and fungal) abundance, fungal diversity and potential heterotrophic respiration than bare microsites, likely due to enhanced litter and sediment redistribution. However, at humid and transition systems, microsites controlled soil N pools and microbial diversity, suggesting tight linkages between vegetation patches and soil microorganisms responsible for N availability. These findings provide evidence of the strong negative impacts of aridification on vegetation attributes and nutrient cycling in coastal dunes and highlight the role of the biotic cover in preserving soil fertility, microbial diversity and functioning, particularly in the most arid sites.

1. Introduction

Climate change is increasing the aridity in many areas of the planet and accelerating the expansion of drylands (Cherlet et al., 2018). In dryland ecosystems, increases in aridity affect biological and geochemical processes leading to abrupt and systematic impacts that

---

* Corresponding author.
E-mail address: mjfa@uc.pt (M.J. Fernández-Alonso).

https://doi.org/10.1016/j.geoderma.2021.114952
Received 17 September 2020; Received in revised form 12 January 2021; Accepted 18 January 2021
Available online 6 February 2021

sequentially endanger productivity, soil fertility and biodiversity (Berdugo et al., 2020). While climate exerts a major influence on dryland functioning at large-scales, the ubiquitous spatial heterogeneity of the biotic cover in natural ecosystems simultaneously controls soil properties, microbial communities and their interactions at local scales, likely modulating climate effects (Okin et al., 2015; Zuo et al., 2010). Previous studies suggest that vascular plants and biological soil crusts might dampen the negative effects of increasing aridity on dryland functioning (Delgado-Baquerizo et al., 2016; Durán et al., 2018; Ochoa-Hueso et al., 2018), but we still lack a detailed understanding of the balance between the effects of broad-scale aridification and the influences of local vegetation cover on the attributes and functioning of drylands. This knowledge is essential to predict the ecological consequences of aridification and has practical implications for ecosystem conservation and management (Ochoa-Hueso et al., 2018).

Climate and edaphic conditions shape attributes of plants and biological soil crusts such as total cover, predominance of functional traits, richness and diversity (Delgado-Baquerizo et al., 2016; Ding and Eldridge, 2020; Ochoa-Hueso et al., 2018). Climate change-driven shifts in plant and biological soil crust communities may trigger cascade effects of different magnitude in other biotic (e.g. soil microbial communities) and abiotic factors (e.g. soil pH, nutrient pools) and processes that operate at different rates, trophic levels and spatial or temporal scales (Berdugo et al., 2020; de Graaff et al., 2014; Okin et al., 2015; Zuo et al., 2010). Recent studies show that increases in aridity are associated with increases in soil biocrust variability, decreases in plant cover, soil C content, fertility, microbial diversity and abundance and biogeochemical processes (Ding and Eldridge, 2020; Maestre et al., 2015, 2012). Similarly, reductions in plant cover as a function of aridity may decouple nutrient cycles and unbalance the ecosystem stoichiometries (Delgado-Baquerizo et al., 2013). Although these ecological patterns are described for drylands at global scale, we still need further insights into the role of the local biotic cover as modulator of the ecosystem responses to aridification in natural systems, especially in those subjected to a climate transient between humid and arid sites.

The positive effects of the biotic cover, including plants and/or biological soil crusts, on biogeochemical processes compared to bare ground interspaces are related to their ability to enhance sediment and water capture, buffer extreme temperatures and solar radiation, and attract a range of biota whose mutual relationships may increase soil fertility and functioning (de Graaff et al., 2014; Okin et al., 2015). These positive effects will likely rely on ecosystem features such as the vegetation type (e.g. canopy architecture, ability to form associations with rhizobacteria), number, composition and size of the biotic patches, connectivity (e.g. water and aeolian transport), and the degree of aridity (e.g. not significant effects have been detected so far in dry-subhumid and humid areas) (Delgado-Baquerizo et al., 2016; Durán et al., 2018; Ochoa-Hueso et al., 2018; Okin et al., 2015). In this respect, the effects of plant and biocrust patches may be particularly important in dune systems as a result of the high aeolian transport, relatively low microbial activity and nutrient availability of their sandy soils.

Coastal dune ecosystems are priority conservation areas due to their significant contribution to global biodiversity holding numerous endemic species, and their capacity to mitigate the impacts of the increasingly frequent extreme climatic events (Mikkonen and Moilanen, 2013; Mo et al., 2020). The Atlantic coastal dunes of the Iberian Peninsula are particularly sensitive to climate change and current projections suggest that these areas will cross aridity thresholds likely compromising their capacity to provide essential ecosystem services (Berdugo et al., 2020). These coastal dune systems represent an exceptional opportunity to carry out a field-based observational study assessing the integrative impacts of increasing aridity and the biotic cover on ecosystem attributes and functioning, because of their patchy spatial pattern and the homogeneity of the soil type along their natural climate gradient.

We aimed to assess how and why major biotic (e.g. total cover, soil microbial abundance and diversity) and soil abiotic (e.g. soil pH, nutrient contents) attributes and functions (e.g. soil mineralization and greenhouse gas fluxes) vary in 24 dune systems distributed along an aridity gradient in the Atlantic coastline of the Iberian Peninsula. To that end, we used an integrative approach. First, we evaluated how aridity affects plant and biocrust communities as well as soil attributes and functions of coastal dunes at a regional scale using a natural climate gradient. Then, we assessed to what extent soil attributes and functioning rates differ between three types of biotic cover (hereinafter called microsites: bare soil, biocrust and plants) at local scale. We hypothesized that (i) aridity shapes the structure of the biotic community decreasing its percentage cover and increasing plant individual sizes; (ii) rates of soil biogeochemical processes would decrease with increasing aridity as a result of the detrimental effects on the soil biotic cover and microbial communities; and (iii) plants and biocrust would promote soil fertility compared to bare ground areas, with these positive effects becoming more relevant as aridity increases.

2. Materials and methods

2.1. Study sites and climate data

Field data were gathered from 24 stabilized coastal dunes across a northwest-to-southeast geographic gradient of increasing aridity along ~1500 km in the coastline of Portugal and Spain (Fig. 1, Table S1). All soils were classified as Arenosols with little profile differentiation and loamy sand texture or coarser, originated by the aeolian sand movement from the beach (IUSS Working Group WRB, 2015). Stabilizing vegetation primarily consisted of creeping grasses (*Ammophila arenaria* (L.) Link), dwarf shrubs (*Helichrysum picardii* Boiss. & Reut.) and suffruticous chamaephytes (*Crucianella marítima* L.), with biological soil crusts and occasional arboreal vegetation (*Pinus pinaster* Aiton and *Pinus pinea* L.) in less arid locations (see García-Velázquez et al., 2020 for more information about perennial vegetation species). In the study sites, the biotic cover and thus the degree of dune stabilization decrease towards the more arid south-east (Table S1).

The climate classification of the study sites is based on the UNEP Aridity Index (AI) calculated as the ratio between precipitation and potential evapotranspiration. The value of the AI for each site was obtained from the Global Aridity Index and Potential Evapotranspiration Climate Database version 2 (Trabucco and Zomer, 2019), while mean annual precipitation (MAP) and temperature (MAT) values were obtained from the WorldClim dataset version 2 (Fick and Hijmans, 2017). These spatially interpolated climate data are aggregated over the reference period of 1970–2000 and has approximately 1-km^2 spatial resolution. The aridity gradient in our study encompassed non-drylands in the north-west of the Iberian Peninsula ($AI \geq 0.65$) and three subtypes of drylands in the south and south-east: dry subhumid ($0.5 \leq AI < 0.65$), semi-arid ($0.2 \leq AI < 0.5$) and arid ($AI < 0.2$) (Cherlet et al., 2018). Mean annual temperature and MAP range from 13.9 to 18.8 °C and from 225 to 1441 mm, respectively. Along the transect, MAT was negatively correlated with MAP (Spearman's rank correlation, $\rho = -0.85$, p-value < 0.001, Fig. S3). We used 1-AI as our surrogate of aridity to facilitate the interpretation of our results.

2.2. Experimental design and data collection

Data collection took place during the dry season in July 2016 and followed a standardized sampling protocol. In each sampling site, a square plot (30 × 30 m) was established parallel to the coastline. In each plot, the percentage cover and composition of plant species were determined using the line-point intercept method (Herrick et al., 2017). Point data were systematically collected every 20 cm along 4 parallel transects of 25-m length. We also counted the number of species present within the square plots to estimate plant richness and measured the height and width of plant individuals.

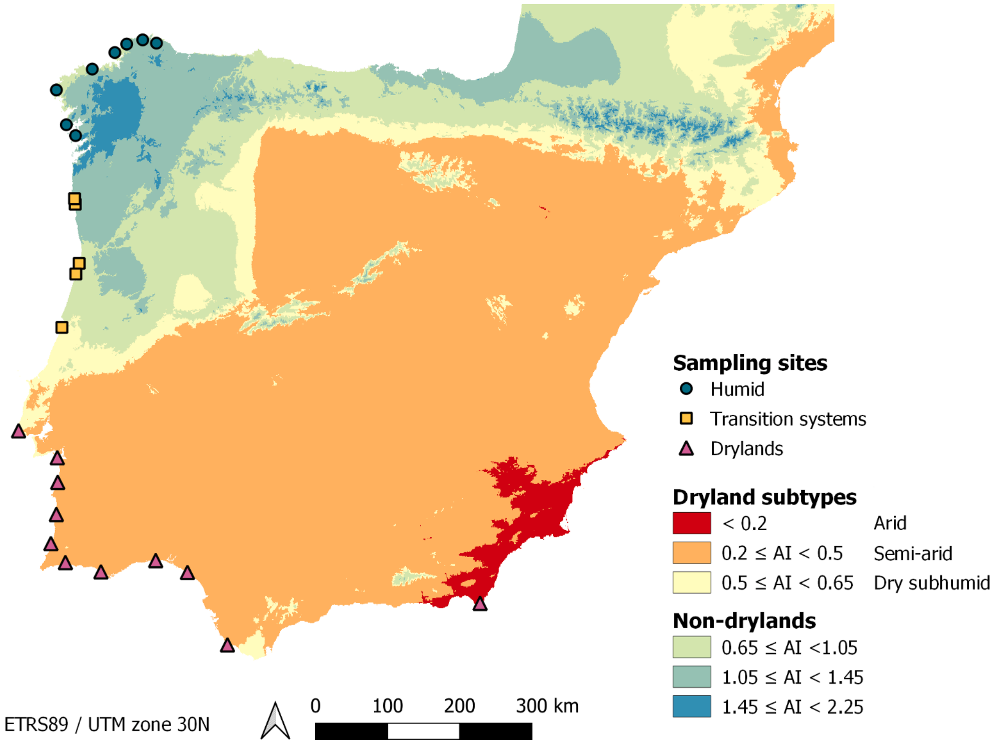

Fig. 1. Sampling transect of 1500 km distributed along an aridity gradient in the Atlantic coastline of the Iberian Peninsula. A total of 24 dune systems were selected. Coloured shapes represent bioclimatic areas of the surveyed dune systems (green circles: humid, yellow squares: transition systems, pink triangles: drylands). Climate classification based on the Aridity Index (AI) is depicted in different colours. Data source for aridity index: (Trabucco and Zomer, 2019) (http://www.cgiar-csi.org).

In the surveyed coastal dunes, we identified three diverse surface microsites according to the patchy configuration of the biotic aboveground communities: vascular plants, biocrust –biological soil crusts with mosses and lichens– and bare soil –open areas devoid of photosynthetic cover–. We performed a stratified random sampling in each microsite, collecting five soil samples from a depth of 0–10 cm and using a square sampler (10 × 10 cm). Soil samples for each microsite were pooled and homogenized to obtain composite samples. Samples were immediately sieved (<2 mm) and divided in two subsamples. One subsample was stored at −80 °C until molecular analysis, and the other one was air-dried in the laboratory and properly stored until carrying out the rest of the analyses.

We classified the 24 dunes sites into three bioclimatic areas: humid areas, drylands and the transition between the two. This classification was based on the magnitude of dunes local heterogeneity, measured as structural attributes (i.e. vegetation percentage cover and type of microsites present), the geographical location along the aridity gradient and the background climate (i.e. AI) (Fig. 1, Table S1). Hence, the *Humid sites* (n = 8), located in the northern part of the aridity gradient, are characterized by plant and biological soil crusts with almost no bare soil. The *Transition sites* (n = 5), located in the mid part of the aridity gradient, included dunes with the three microsites clearly identified. Lastly, the *Drylands* (n = 11), located in the southern and eastern part of the gradient, include plots having only plant and bare soil microsites.

2.3. Soil properties and functions

Soil pH was analysed with a calibrated pH-meter at a suspension ratio of 1:2.5 (weight:volume) in water. Soil water-holding capacity (WHC) was determined by the percolation method (Harding and Ross, 1964). Soil organic matter content was estimated by loss-on-ignition (450 °C for 4 h; Nelson and Sommers, 1996). Soil total carbon (C) and nitrogen (N) were determined by dry combustion using a TruSpec CN analyser (LECO Corp., St. Joseph, MI, USA). Soil inorganic C was analysed by the volumetric method using a Bernard calcimeter (Pansu and Gautheyrou, 2006). Soil organic C (OC) was determined by difference between total C and inorganic C. Soil extracts with 1 N KCl (1:5, weight:volume) were analysed for total inorganic N (NH_4^+-N and NO_3^--N concentrations) using a modified blue indophenol colorimetric method with Devarda's alloy (Sims et al., 1995) and a microplate reader (Heales, Shenzhen, China) as in Rodríguez et al. (2009). Dissolved organic N (DON) was estimated by subtracting total inorganic N from total extractable N determined both in same soil-K_2SO_4 extracts (Rodríguez et al., 2009). Briefly, soil samples were extracted with 0.5 M K_2SO_4 (1:10, weight:volume) and analysed for total extractable N using the persulfate oxidation technique (D'Elia et al., 1977) and total inorganic N as described above. Total phosphorus (P) was calculated as the sum of all the fractions sequentially extracted from 0.5 g of air-dried soil following the method by Tiessen and Moir (2006), which is a modified version of the Hedley fractionation technique (Hedley et al., 1982; see García-Velázquez et al., 2020 for the detailed protocol), and determined by the malachite green method (Fernández et al., 1985; modified from Hess and Derr, 1975) in a Jupiter microplate reader (Asys Hitech GmbH, Eugendorf, Austria). Soil ratios for OC:N, OC:P and N:P were calculated. Analytical results for soils were expressed on a soil dry-weight basis (oven-drying a subsample at 105 °C to constant mass), except for WHC.

Potential heterotrophic respiration and N mineralization rates were measured in 100 g of air-dried soil incubated in darkness during 13 days with optimal conditions of temperature and moisture (25 °C and 60% of WHC). Measurements of soil CO_2 efflux were taken in days 0, 1, 2, 3, 4, 7, 9, and 13 days of incubation using glass jar chambers (1 L volume) and the closed dynamic chamber method (Pumpanen et al., 2004). Chambers were closed and connected to an infrared gas analyser EGM-4 (PP-System, Hertfordshire, United Kingdom). The increase in headspace CO_2 concentration was recorded during 60 s at 5-second intervals from one minute after the lid closure to discard fluctuations. Potential heterotrophic respiration rates were calculated as the linear increase in CO_2 concentration, averaged for the incubation period and expressed as g

kg^{-1} day^{-1} of dry weight soil by using the ideal gas law equation (Rodríguez et al., 2019). Potential N mineralization rates were calculated as the net increase in total inorganic N over the incubation period by comparing soil NH_4^+-N and NO_3^--N concentrations in the soil samples before and after the incubation period (Rodríguez et al., 2019). Potential net N mineralization rates were expressed as mg kg^{-1} day^{-1} of dry weight soil.

One composite soil sample per site was created by mixing a weight of discrete air-dried soil sample from each microsite as a function of its respective percentage cover. Composite soil samples (60 g) were incubated into 0.5 L glass jars in darkness and with optimal conditions of temperature and moisture (25 °C and 60% of WHC). The closed static chamber method (Pumpanen et al., 2004) was used to estimate potential rates of greenhouse gas fluxes (CO_2, CH_4 and N_2O) 1, 2, 3, 5, 8 and 10 days after the incubation. Headspace gas was sampled at 0 and 60 min after the jars closure through a rubber septum fitted in the lid. Before removing the samples, the gas in the headspace was gently pumped up and down with a syringe three times to guarantee the homogenization. Then, gas samples were collected with the syringe, transferred to 22 ml pre-evacuated glass vials and kept at room temperature until analysis. The N_2O, CO_2 and CH_4 concentrations in air gas samples were determined in a gas chromatograph GC-2014 (Shimadzu, Japan) connected to a headspace autosampler HS20 (Shimadzu, Japan) and equipped with an ^{63}Ni electron capture detector, a thermal conductivity detector and a flame ionization detector. Rates of greenhouse gas fluxes were calculated as the linear increase in gas concentration over the chamber closing time, averaged for the incubation period and expressed as mg kg^{-1} day^{-1} or μg kg^{-1} day^{-1} of dry weight soil by using the ideal gas law equation.

2.4. Soil microbial abundance and diversity

Soil DNA was extracted from 0.5 g of each soil sample using the PowerSoil DNA isolation kit (MOBIO Laboratories, Inc. Carlsbad, CA, USA). We followed the manufacturer's instructions, except for the utilization of a tissue homogeniser (Precellys 24-dual, Bertin technologies, Montigny-le Bretonneux, France) twice, for 45 s at 4500 rpm in the lysis step. Soil bacterial and fungal abundances in extracted DNA subsamples were determined using Real-time quantitative PCR (q-PCR) in 96-well plates on an ABI 7300 Real-Time PCR (Applied Biosystems, Foster City, CA. USA). We used primers pairs Eub338/Eub518 for bacterial 16S rRNA genes and ITS1F/5.8 s for fungal ITS (Internal Transcribed Spacer) region (Fierer et al., 2005; Maestre et al., 2015). The qPCR assays were performed in duplicate 10-μl PCR reaction mixtures containing 2 μl of DNA template (4 ng $μl^{-1}$), 5 μl of PowerUp SYBR Green Master Mix (2x) (Applied Biosystems, Foster City, CA, USA), 0.3 μl of each primer (0.4 mM) and 0.4 μl of bovine serum albumin (0.4 mg ml^{-1}).

Subsamples of soil metagenomic DNA were used for the microbial community profiling using the Illumina MiSeq platform after PCR amplification with the primer sets 341F/805R (Herlemann et al., 2011) for the bacterial 16S rRNA gene and FITS7/ITS4 (Ihrmark et al., 2012) for the fungal ITS regions. Raw pair-end reads were trimmed by cutting off the barcode and primer sequences using USEARCH (Edgar, 2010). Default merging parameters were employed and sequences were quality filtered to a maximum expected error threshold of 0.8. Sequences were denoised and clustered into zero-radius operational taxonomic units (zOTUs) using UNOISE3 (Edgar, 2016). Taxonomic assignment of $_{Z}$OTUs was performed in QIIME (Caporaso et al., 2010) against the SILVA database (http://www.arb-silva.de/) for bacterial taxa. Fungal taxa were annotated in QIIME against the UNITE database (https://unite.ut.ee/) using BLAST. Approximately, 2.6 M and 2.5 M high-quality merged-sequences were mapped for zOTU in bacteria and fungi, respectively. The resultant zOTU abundance tables were rarefied to an even number of sequences per sample to ensure an equal sampling depth (14,187 and 18,924 for bacteria and fungi, respectively) and then converted into a Biological Observation Matrix (BIOM) format files. BIOM files were imported into QIIME for the calculation of alpha diversity indexes including richness (zOTU counts), Simpson's evenness, Shannon diversity, and Faith's phylogenetic diversity.

2.5. Data analysis

Data for all soil variables, except for the greenhouse gas fluxes, were averaged to obtain site-level estimates ($n = 24$) by using the values observed in each microsite (i.e. plants, biocrust and bare soil) weighted by their respective percentage cover at each site. Then, we explored the linear or quadratic relationships of aridity, MAP and MAT with plant community attributes, soil physicochemical properties and microbial diversity and abundance. Similarly, we assessed the relationship between climate variables and soil biogeochemical processes (potential greenhouse gas fluxes, heterotrophic respiration and N mineralization rates). We used generalised linear models with gamma error distribution and the inverse link function when necessary to satisfy the normality assumption. After inspected for outlier observations, we compared alternative models using the Akaike Information Criterion corrected for small samples sizes (AICc, Burnham and Anderson, 2002). Models with $\Delta AICc > 10$ indicate that the worst model has essentially no support and can be omitted from consideration (*MuMIn* package, Barton, 2018). We conducted a heatmap representation of the Spearman's rank correlation matrix among the studied variables (*corrplot* package, Wei and Simko, 2017).

We evaluated the effects of microsites on soil physicochemical and biological properties using separated linear mixed effect (LME) models for each bioclimatic area (i.e. humid sites, transition sites, drylands). In all LME models we included 'sampling site' as a random factor given that data arises from a stratified design (*nlme* package, Pinheiro et al., 2017). Models were inspected for the general assumptions of normality and homoscedasticity. Tukey's honestly significant differences of least-square means (*lsmeans* package, Lenth, 2016) were performed whenever significant factor effects of microsites were detected.

All the analyses and figures were carried out in the statistical platform R version 3.4.0. (R Core Team, 2019). The significance level was 0.05 for all the analyses.

3. Results

3.1. Climate effects on plant and biocrust communities

Our results indicate that aridity (1-AI) affects structural attributes of coastal dunes at a regional scale. Total biotic cover and plant width responded in a non-linear manner to increases in aridity (Fig. 2). Specifically, increases in aridity only drove substantial decreases in the biotic cover once an aridity threshold was reached (Fig. 2a, vertex at an aridity value of −0.04). Hence, total cover decreased at the point where precipitation equalled potential evapotranspiration. On the contrary, increasing aridity beyond an aridity threshold caused significant increases in plant width (Fig. 2b, vertex at an aridity value of 0.17). The remaining analysed plant community attributes were not significantly influenced by aridity (Table S2). Plant richness showed a significantly negative quadratic relationship with MAT clearly separating humid and transition sites from drylands (Fig. S1a, Table S2). Plant height significantly increased with decreasing MAP, although with a relatively low explained deviance (Fig. S1b, Table S2).

3.2. Climate effects on soil attributes and functioning

We detected consistent decreasing patterns of soil physicochemical and microbial attributes along the natural aridity gradient in the coastal dune systems (Fig. 3). Thus, soil WHC, soil organic matter, total N and P concentrations significantly decreased with increasing aridity (Fig. 3a-d). However, soil pH, OC and inorganic C, DON, total inorganic N and soil stoichiometric ratios were neither significantly responsive to

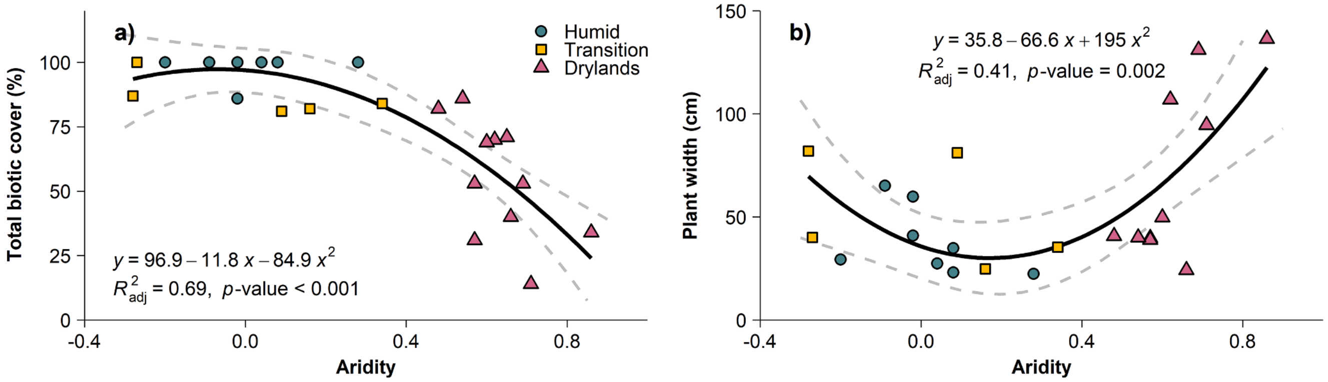

Fig. 2. Quadratic relationships of a) total biotic cover (%) and b) plant width (cm) with aridity (expressed as 1-AI) at the dune sites. Coloured shapes indicate dune sites classification according to bioclimatic areas (green circles: humid, yellow squares: transition systems, pink triangles: drylands). The black solid line and the dashed grey lines represent the fitted regression and the 95% confidence interval, respectively. The adjusted R^2 (R^2_{adj}) values were used as a measure of goodness-of-fit of the models.

increases in aridity (Table S3). Moreover, our results indicate that increases in aridity inhibited potential N mineralization mainly through decreased nitrification rates, since ammonification was unresponsive to increasing aridity (Fig. 3e and S2a, Table S3). However, we did not find significant patterns for potential soil CO_2 (Fig. 3f), CH_4 nor N_2O fluxes along the aridity gradient (Table S3). Our results further showed that increases in aridity significantly reduced soil bacterial abundance (Fig. 3g), bacterial richness (Fig. 3h), bacterial diversity (Shannon index, Fig. S2b) and both bacterial and fungal phylodiversity (Faith's) (Fig. 3i-j). We did not find significant relationships between aridity and soil fungal abundance, fungal richness, fungal diversity (Shannon) and both bacterial and fungal evenness (Simpson's) indices (Table S3).

3.3. *Effects of microsites on soil attributes and functioning*

Our results indicate that soil physicochemical properties and biogeochemical functions differ between cover types (i.e. microsites) and that these differences were dependent on the degree of aridity (Table S4). In drylands, soils beneath vascular plants had higher WHC than those from bare ground areas (Fig. 4a). Similarly, soils under plants consistently had higher soil OC and organic matter than those located in bare ground interspaces, but these differences were only significant at the most arid dune systems (Fig. 4b, Table S4). Interestingly, we found significant differences in N-related variables between microsites only in humid and transition sites. In humid sites, soils beneath biocrust showed higher contents of total inorganic N than those beneath vascular plants (Fig. 4c), whereas in transitions sites soils beneath plants showed higher concentrations of DON than those beneath biocrust and from bare areas (Fig. 4d). Regarding soil functioning, soils beneath vascular plants tended to show higher potential heterotrophic respiration than bare soils although, once again, these differences were only significant for dryland sites (Fig. 4f). Potential N mineralization was rather similar among microsites in all dune sites (Fig. 4e).

Soil microbial diversity and abundance were differently controlled by microsites at local scale (Table S4). We detected greater abundances of both bacteria (Fig. 5a) and fungi (Fig. 6a) in soils collected under vascular plants than in bare ground areas, but this pattern was only statistically significant in drylands. On the contrary, bacterial alpha diversity –Shannon index, richness and phylodiversity– showed to be more sensitive to microsites in transition and humid sites than in drylands (Fig. 5b, c and e), with levels decreasing in the following order: vascular plants, biocrust and bare soil. Soil fungal communities showed similar decreasing patterns for all alpha diversity indices but in this case differences among microsites were significantly different regardless of the bioclimatic area (Fig. 6b, c and e). Bacterial and fungal evenness were similar among microsites in all bioclimatic areas (Figs. 5d and 6d).

4. Discussion

Our findings show that coastal dune ecosystems are sensitive to increases in aridity and may experience detrimental effects on the biotic cover (e.g. reductions in total cover and shifts towards shrub-dominated patches) and soil attributes (e.g. reductions in soil organic matter, microbial diversity, total N and P) with negative consequences for biogeochemical processes (e.g. reductions in potential N mineralization). These findings coincide with an extensive literature studying the effects of aridification worldwide (Berdugo et al., 2020; Delgado-Baquerizo et al., 2013; Maestre et al., 2015, 2012). However, few studies have been designed to simultaneously assess the effects of aridity and microsites beneath the biotic cover (i.e. vascular plants and/or biological soil crusts) on soil attributes and functioning in a broad range of aridity conditions with soils that share the same development origin and are relatively homogeneous in properties along and between soil profiles. Our integrative approach using a natural climate gradient at regional scale coupled with the use of microsites at local aridity levels in which important changes could be expected to occur –transition between drylands and humid sites– allowed us to show that microsites may interact with aridity to determine soil fertility, microbial diversity and functioning.

4.1. *Aridity negatively affects the biotic cover and soil attributes*

Our results revealed that climate change may drive shifts in the aboveground biotic community of the Atlantic coastal dunes through decreases in MAP and increases in MAT and aridity. As we hypothesized, total biotic cover decreased with increasing aridity but only when dune systems were exposed to potential water scarcity (i.e. once potential evapotranspiration equalled precipitation in the aridity gradient). We further confirmed that reductions in the biotic cover might be accompanied by shifts in plant community composition and structure favouring species and individuals of larger sizes (i.e. greater widths and heights in response to increases in aridity and decreases in MAP, respectively). These results are consistent with recent field surveys referring reductions in total cover and greater importance of plant patches dominated by shrub species in response to aridification around the world (Berdugo et al., 2020; Ochoa-Hueso et al., 2018). In our climate gradient, the vegetation shift towards shrub-dominated communities surrounded by bare soil seems to be abrupt between transition sites and drylands (indicated by non-linear relationships between the biotic cover attributes and climate drivers). This shift in the vegetation structure at drylands may be sustained by positive feedbacks between shrubs and environmental conditions improving soil properties, such as the protection of soil moisture, and the improvement of the nutrient retention

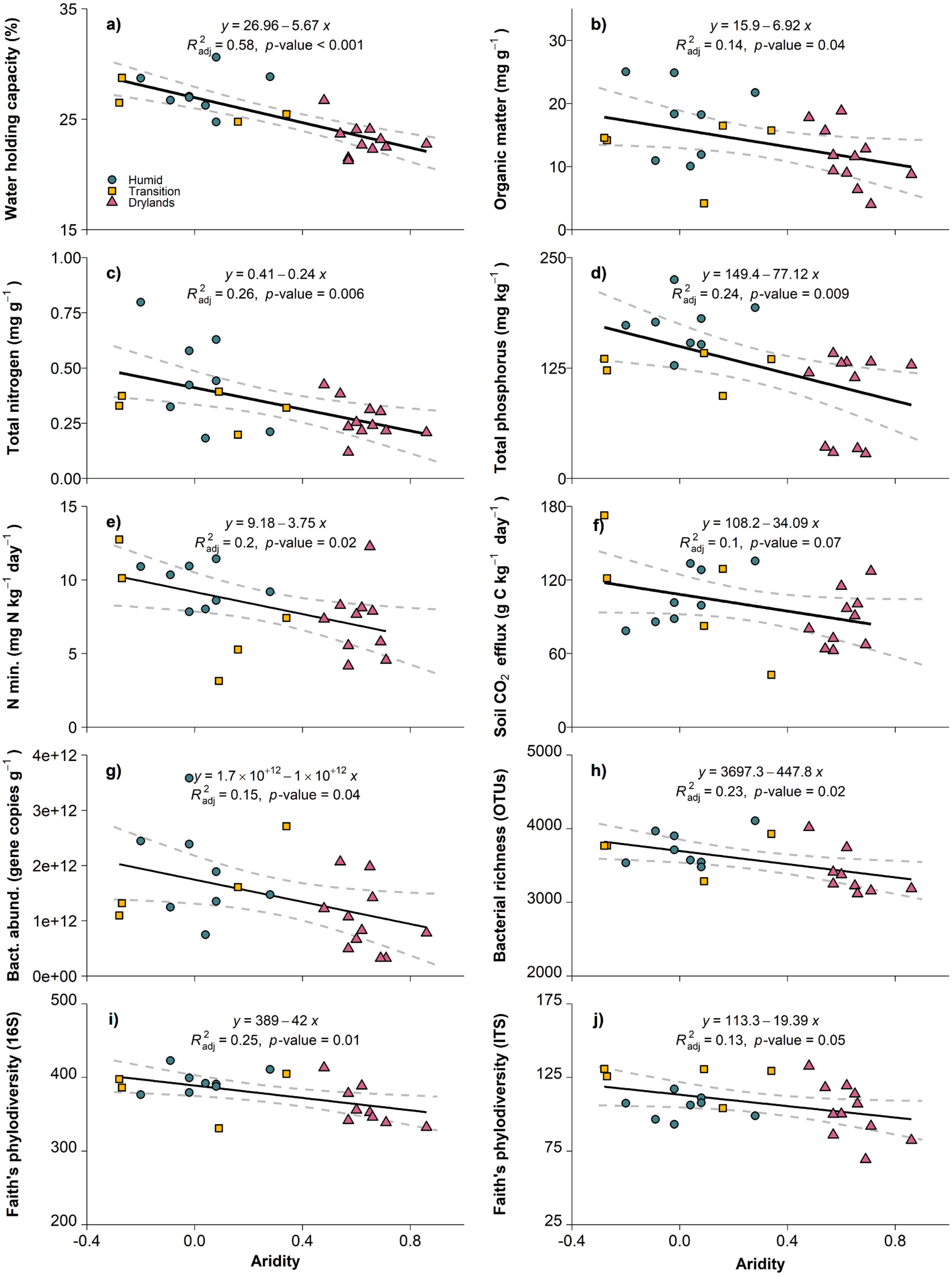

Fig. 3. Relationships of soil physicochemical properties (a-d), biogeochemical functions (e, f), microbial abundance and diversity (g-j) with aridity (expressed as 1-AI) at the dune sites. Coloured shapes indicate dune sites classification according to bioclimatic areas (green circles: humid, yellow squares: transition systems, pink triangles: drylands). The black solid line and the dashed grey lines represent the fitted regression and the 95% confidence interval, respectively. The adjusted R^2 (R^2adj) values were used as a measure of goodness-of-fit of the models. N min, potential nitrogen mineralization; Bact. abund., bacterial abundance.

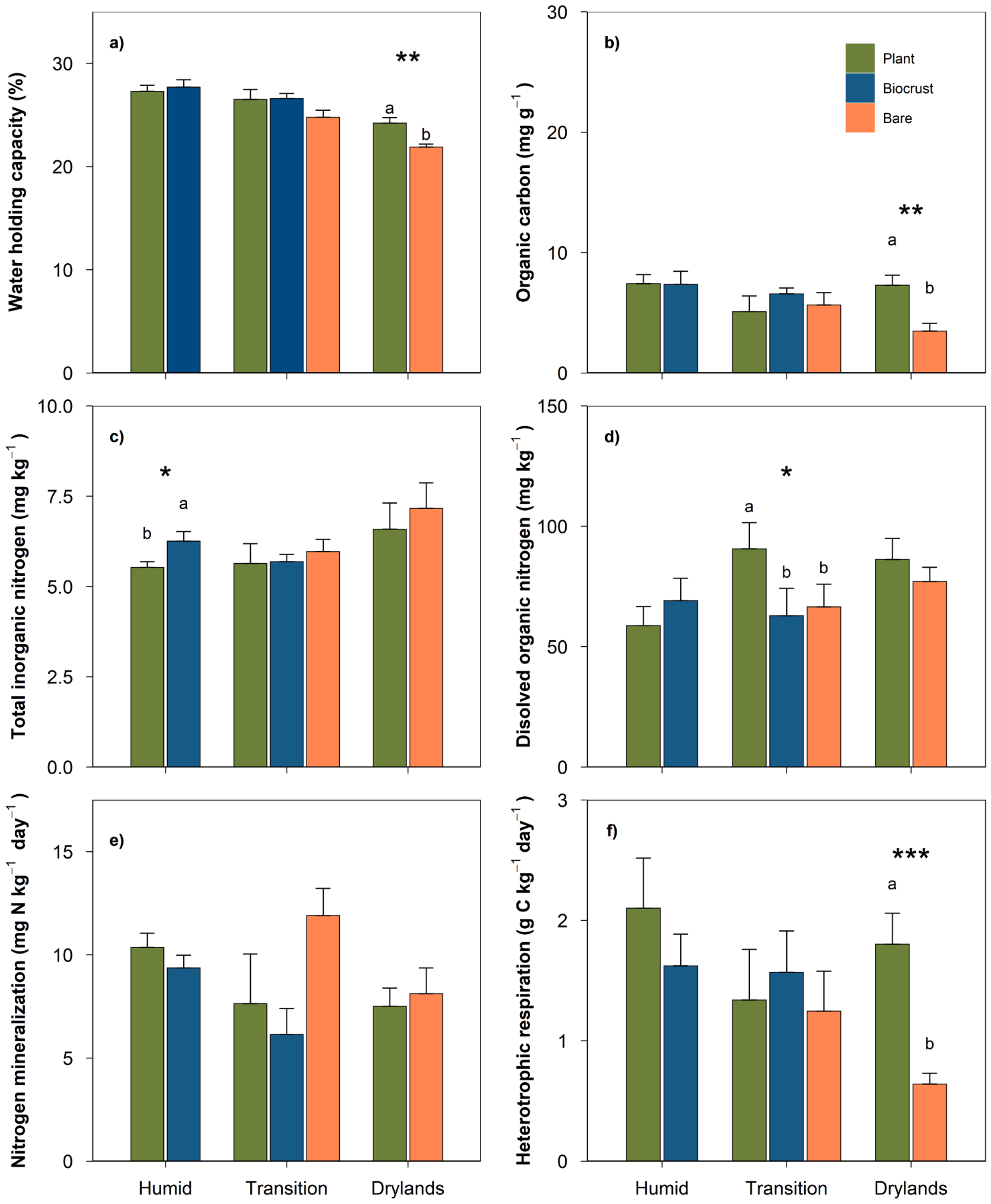

Fig. 4. Changes in soil physiochemical properties (a-d) and functions (e-f) between microsites (green: plant, blue: biocrust, orange: bare soil) at the dune sites classified as Humid areas, Transition areas and Drylands, according to bioclimatic areas. Bars represent means ± standard errors. Small letters denote significant differences between microsites (LME models). Significance levels: (***) $p < 0.001$, (**) $p < 0.01$, (*) $p < 0.05$.

capacity and soil texture (D'Odorico et al., 2012). Moreover, we detected contrasting effects of increasing MAT on plant richness between humid –positive effects– and arid sites –negative effects–. Whereas temperature is generally a positive driver of plant species richness (Pausas and Austin, 2001), the strong decline in our dune sites beyond a MAT value (~16 °C) could be associated with a major turnover in species selecting a few physiological and functional strategies able to cope with harsh arid conditions (Berdugo et al., 2020; Ulrich et al., 2014).

As we stated in the second working hypothesis, climate change-driven shifts in vegetation attributes may subsequently affect soil properties negatively affecting soil biogeochemical processes and fertility. The aboveground biotic components are known to play a key role in dune stabilization reducing soil erosion, promoting finer soil textures and favouring the accumulation and stability of soil organic matter (Li et al., 2007; Plaza et al., 2018; Zuo et al., 2010). In our study, reductions in total biotic cover with increasing aridity were linked to concomitant decreases in soil WHC and organic matter content, which are likely behind the observed decreases in soil microbial (bacterial and fungal) diversity and functioning –e.g. potential soil N mineralization– (Linstädter and Baumann, 2013; Maestre et al., 2015, 2012). Interestingly, soil bacterial abundance was more sensitive to increasing aridity

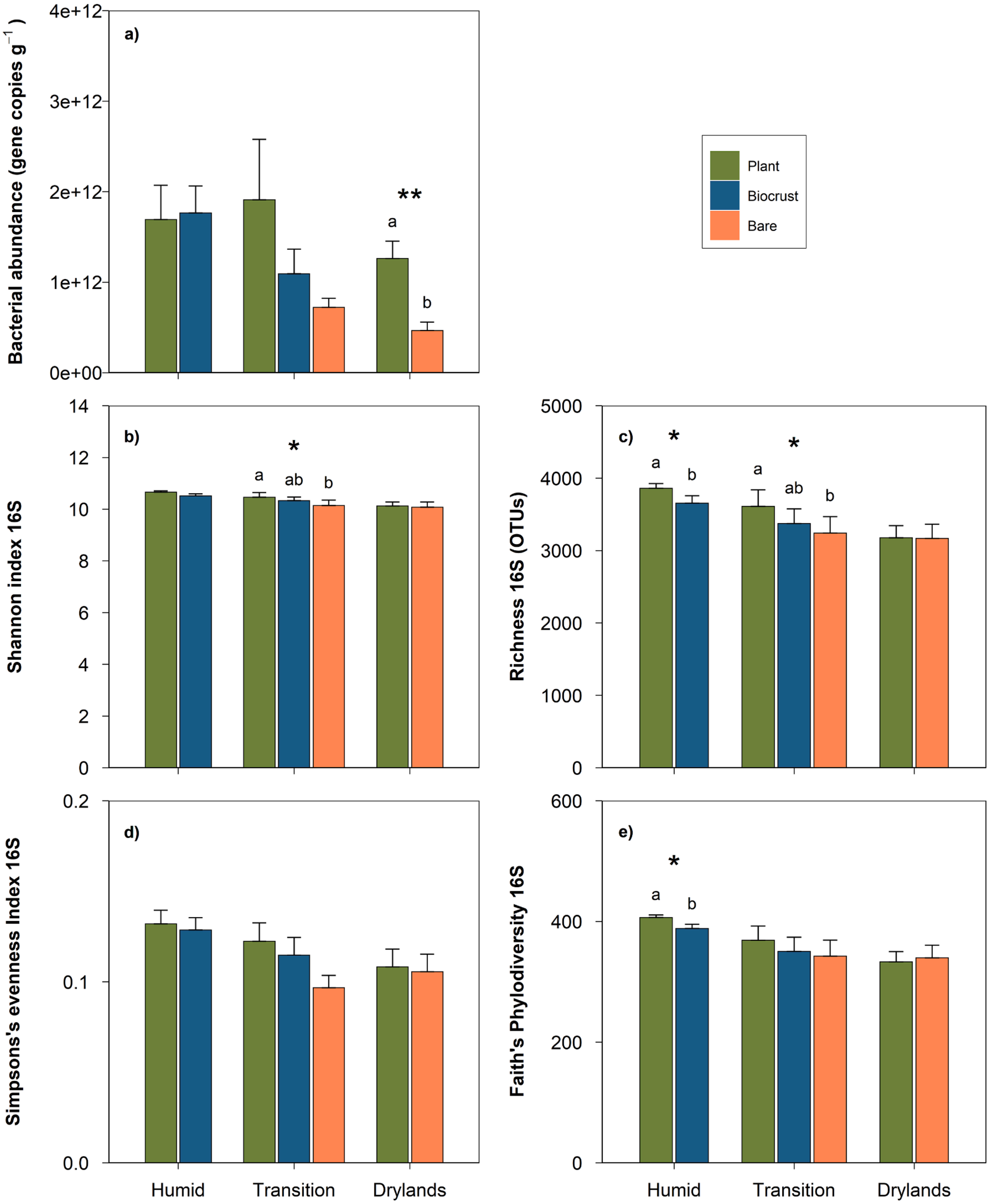

Fig. 5. Changes in (a) abundance and (b-e) alpha diversity of soil bacterial communities between microsites (green: plant, blue: biocrust, orange: bare soil) at the dune sites classified as Humid areas, Transition areas and Drylands, according to bioclimatic areas. Bars represent means ± standard errors. Small letters denote significant differences between microsites (LME models). Significance levels: (**) $p < 0.01$, (*) $p < 0.05$.

than fungal abundance, maybe due to the several response traits (e.g. sporulation or cell wall architecture) that confer fungal organisms resistance and resilience to climate change-associated disturbances such as drought (de Vries et al., 2020).

Because soil OC, N and P availability are tightly linked to biological productivity and activity (Delgado-Baquerizo et al., 2013; García-Velázquez et al., 2020; Wang et al., 2020), we would expect that increasing aridity would deplete both soil OC and nutrient pools. In our dune soils only total N and P significantly declined along the aridity gradient. We speculate that the shift in the vegetation structure towards shrub-dominated dunes with increasing aridity may cause a net reduction in the quality of plant litter entering the soil (i.e. higher litter OC:N ratios) affecting microbial communities and C and N turnover rates at different extents (Fernández-Alonso et al., 2018; Rodríguez et al., 2017). The reduced chemical weathering by precipitation might explain the tendency towards a decrease in total P with increasing aridity (García-Velázquez et al., 2020). In any case, the differential sensitivity to changes in aridity of OC, N and P pools could lead to a decoupling between soil nutrient cycles in these systems (Li et al., 2007; Schimel and Bennett, 2004), with likely important but hard to anticipate effects on ecosystem functioning (Delgado-Baquerizo et al., 2013; Finzi et al., 2011).

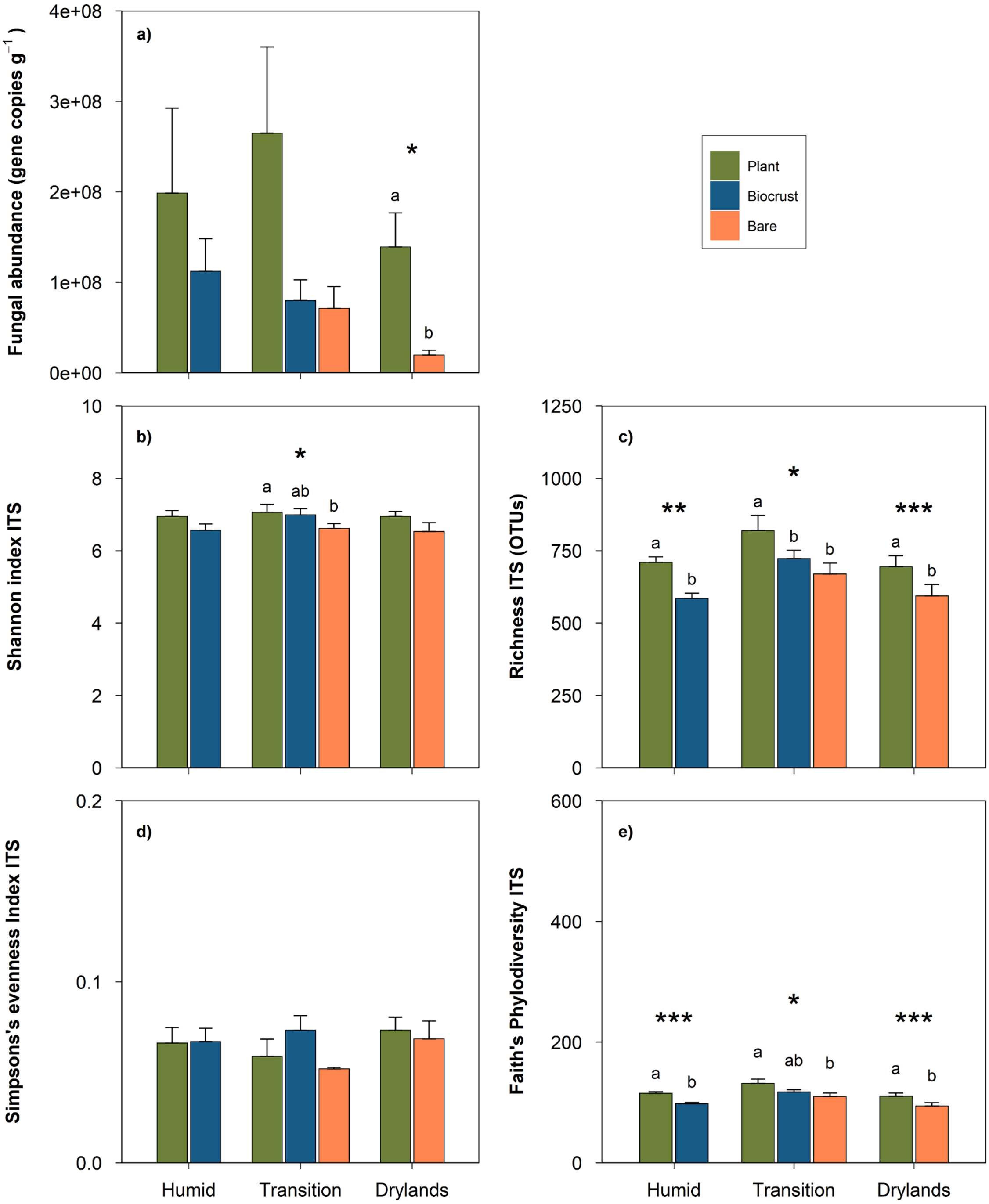

Fig. 6. Changes in (a) abundance and (b-e) alpha diversity of soil fungal communities between microsites (green: plant, blue: biocrust, orange: bare soil) at the dune sites classified as Humid areas, Transition areas and Drylands, according to bioclimatic areas. Bars represent means ± standard errors. Small letters denote significant differences between microsites (LME models). Significance levels: (***) $p < 0.001$, (**) $p < 0.01$, (*) $p < 0.05$.

Interestingly, we did not find significant patterns of inorganic C and soil pH along the aridity gradient, even though aridity generally tends to reduce the losses of dissolved salts by leaching leading to the accumulation of calcium carbonate and silicate dust and to relatively high pH values (Ewing et al., 2006; Plaza et al., 2018). We suggest that the spray of seaborn salt –a characteristic process of coastal dunes (Clayton, 1972; Sevink, 1991– could be affecting soil salinity and pH to a greater extent than climate in the studied dune systems. Our results stress that different abiotic factors such as aridity and seaborn spray, both of which are likely to be affected in coming decades by climate change, may interact and, in some cases, have opposite effects on the dynamics and stability of element forms in coastal dunes (García-Velázquez et al., 2020). Overall, our results highlight that the response of soil fertility and stoichiometry to climate change may be different at global and regional scales as a consequence of landscape-specificity (Wang et al., 2020).

4.2. *Microsites as modulators of the aridity effects on soil attributes and functioning*

Our study provides empirical evidence that microsites control soil physicochemical properties, microbial attributes and biogeochemical processes at the local scale. Most importantly, our results show that the influence of plants and soil biological crusts on soil attributes is highly dependent on the degree of aridity. Coastal dunes are early successional ecosystems presenting relatively young soils characterized by low nutrient (particularly N and P) and OC (energy) availabilities (Jones et al., 2008; Laliberté et al., 2012). At transition sites, we found a positive effect of plant cover increasing the soil organic N pool with regard to cryptograms or bare soil, likely due to greater root exudation, litter deposition and microbial decomposition of soil organic matter. This spatial pattern for dissolved organic N did not occur in humid sites, suggesting a faster N cycling with both higher N mineralization and uptake rates under the plants of these sites than in transitional areas, mostly driven by better organic matter quality and higher microbial diversity. At humid sites, biocrust increased soil inorganic N accumulation compared to plant canopies suggesting the existence of specific associations with soil bacteria (e.g. *Cyanobacteria*) that enable the atmospheric N fixation, (Delgado-Baquerizo et al., 2016; Elliott et al., 2014; Jones et al., 2008). In our study, the lower soil organic matter content and reduced capacity to retain moisture along the aridity gradient may lead to the disappearance of the biological soil crusts in drylands (Ding and Eldridge, 2020), depriving soils of the biological N fixation processes. It is also important to notice that the sampling depth used in this study (top 10 cm of soil) may have diluted the effects of biocrust on the studied soil attributes and functions given the thin thickness of the biocrust.

At most arid sites, the plant beneficial effects on soil attributes were also present through other mediated processes. As we showed, shifts in the structure of the plant community with increasing aridity followed a quadratic response affecting the connectivity –with decreased biotic cover–, plant richness and individual sizes. Similarly, microsite control of certain soil attributes and processes with increasing aridity could suggest the existence of an abrupt change from which the role of nurse plants in the formation of fertile islands become evident. The establishment of shrub-dominated patches in drylands may suppose a redistribution of materials and resources (e.g. fine-sized mineral particles or litter) through increased deposition and accumulation processes, or reduced soil erosion. Hence, the spatial heterogeneity of plant cover in drylands likely results in greater soil WHC, accumulation of soil organic matter and OC, microbial abundance and potential heterotrophic respiration than in bare soil (de Graaff et al., 2014; Yuan et al., 2012).

Regarding microbial attributes, it is interesting to highlight that differences in the bacterial diversity among microsites were only significant in humid and transition sites, while for the fungal community these differences were independent of the site dryness. This result supports the higher sensitivity of bacteria than fungi to increasing aridity above discussed. Further, it suggests that warmer and drier conditions could favour soil microbial communities richer in fungal taxa, which may eventually have consequences for OC sequestration and stabilization (Curiel Yuste et al., 2011), but also increase the proportion of fungal plant pathogens (Delgado-Baquerizo et al., 2020).

Despite we did not specifically assess the interaction effects between aridity and microsites –the natural dune geographic gradient does not meet a full factorial design–, we may infer under the assumption of space-for-time substitution a sequential role of microsites controlling N-related soil variables at humid and transition sites, and C-related soil variables in drylands. Previous studies have observed asymmetrical responses of biogeochemical cycles and greenhouse gas fluxes to climate change, with microbial communities related to N cycling often being more sensitive than those related to C-cycling (Durán et al., 2018; Fernández-Alonso et al., 2018; Lafuente et al., 2019). Consequently, the transition dune sites may represent the domain where the effects of climate factors on vegetation community are already there but the top-down effects on soil attributes are still not quite significant. Our results provide further evidence of the vulnerability of Atlantic coastal dunes to climate change and the need of practical managements aimed to preserve the native vegetation cover and the natural migration of adapted species to climate changes. This management would be of paramount importance to mitigate the negative ecological consequences of dryland expansion on soil fertility and functioning. Our recommendations are specially encouraged in coastal dunes located in the transition areas which would promptly undergo the observed detrimental effects of increasing aridity.

5. Conclusions

Our study provides evidence that increasing aridity in dune systems may decrease total biotic cover and favour the formation of shrub-dominated patches negatively affecting soil microbial communitites, nutrients, organic matter and N mineralization rates. Interestingly, soil bacterial communities were more sensitive to increases in aridity than fungal communities, which were more influenced by the type of microsite. Our study also provides insights on the important role of the vegetation cover regulating belowground biotic and abiotic attributes in dune ecosystems and, more importantly, highlights the aridity degree as modulator of these effects. Related to this, our results suggest the existence of specific relationships between the biocrust and bacterial taxa fostering N-fixation and transformation processes in dune soils at humid and transition systems, and the formation of fertile islands under shrub microsites in drylands. These findings significantly advance the understanding of the potential effects of climate change-driven dryland expansion on the vegetation community structure and soil functioning of coastal dunes systems and stress the need to preserve the vegetation cover of these ecosystems.

Declaration of Competing Interest

The authors declare that they have no known competing financial interests or personal relationships that could have appeared to influence the work reported in this paper.

Acknowledgements

We thank Antonio Gallardo, Jesús Rodríguez, Felix Durán, and Delia Humia for their help with the logistics during the samplings. We thank Agustín Rubio for the support in soil chemical analysis. This work was carried out at the R&D Unit Center for Functional Ecology - Science for People and the Planet (CFE), with reference UIDB/04004/2020, financed by FCT/MCTES through national funds (PIDDAC). M.J.F.A., J. D. and A.R. acknowledge support from the Fundação para Ciência e Tecnologia (PTDC/BIA-ECO/30231/2017, IF/00950/2014 and SFRH/BDP/108913/2015, respectively). L.G.V. acknowledges support from FEDER/Ministerio de Ciencia, Innovación y Universidades-Agencia Estatal de Investigación/Proyect (CGL2017-88124-R). A. L. acknowledges support from a FPI fellowship from the Spanish Ministry of Economy and Competitiveness (BES-2014-067831). B.K.S. research on biodiversity and ecosystem function relationship is funded by the Australian Research Council (DP170104634). LEAF is funded by Fundação para a Ciência e a Tecnologia (Lisbon, Portugal), through the project (UID/AGR/04129/LEAF/2020).

Data accessibility

The primary data of this study is available on Figshare: https://doi.org/10.6084/m9.figshare.12674375.v1 (Fernández-Alonso et al., 2021).

Authors' contributions

J.D. and A.R designed the study and coordinated field sampling campaigns; J.D, A.R, L.G.V. and E.D.S. collected field data and samples; J.D., A.R., L.M., L.G.V., A.L., E.D.S. and M.J.F.A. conducted laboratory incubations and soil analysis; D.F. carried out chromatography analyses; B.K.S. and J.T. provided the Illumina data and conducted bioinformatics analyses. Data were statistically analysed by M.J.F.A. The paper was written by M.J.F.A. and substantially edited by A.R. and J.D with all co-authors reviewing the subsequent drafts.

Appendix A. Supplementary data

Supplementary data to this article can be found online at https://doi.org/10.1016/j.geoderma.2021.114952.

References

Barton, K., 2018. MuMIn: Multi-Model Inference.

Berdugo, M., Delgado-Baquerizo, M., Soliveres, S., Hernández-Clemente, R., Zhao, Y., Gaitán, J.J., Gross, N., Saiz, H., Maire, V., Lehmann, A., Rillig, M.C., Solé, R.V., Maestre, F.T., 2020. Global ecosystem thresholds driven by aridity. Science 367 (6479), 787–790. https://doi.org/10.1126/science:aay5958.

Burnham, K.P., Anderson, D., 2002. Model Selection and Multimodel Inference: A Practical Information-Theoretic Approach. Springer-Verlag, New York, 10.1007/b97636.

Caporaso, J.G., Kuczynski, J., Stombaugh, J., Bittinger, K., Bushman, F.D., Costello, E.K., Fierer, N., Peña, A.G., Goodrich, J.K., Gordon, J.I., Huttley, G.A., Kelley, S.T., Knights, D., Koenig, J.E., Ley, R.E., Lozupone, C.A., McDonald, D., Muegge, B.D., Pirrung, M., Reeder, J., Sevinsky, J.R., Turnbaugh, P.J., Walters, W.A., Widmann, J., Yatsunenko, T., Zaneveld, J., Knight, R., 2010. QIIME allows analysis of high-throughput community sequencing data. Nat. Methods 7 (5), 335–336. https://doi.org/10.1038/nmeth.f.303.

Cherlet, M., Hutchinson, C., Reynolds, J., Hill, J., Sommer, S., von Maltitz, G. (Eds.), 2018. World Atlas of Desertification. Publication Office of the European Union, Luxembourg. https://doi.org/10.2760/06292.

Clayton, J.L., 1972. Salt spray and mineral cycling in two california coastal ecosystems. Ecology 53, 74–81. https://doi.org/http://www.jstor.org/stable/1935711.

Curiel Yuste, J., Peñuelas, J., Estiarte, M., Garcia-Mas, J., Mattana, S., Ogaya, R., Pujol, M., Sardans, J., 2011. Drought-resistant fungi control soil organic matter decomposition and its response to temperature. Glob. Chang. Biol. 17, 1475–1486. https://doi.org/10.1111/j.1365-2486.2010.02300.x.

D'Elia, C.F., Steudler, P.A., Corwin, N., 1977. Determination of total nitrogen in aqueous samples using persulfate digestion1. Limnol. Oceanogr. 22 (4), 760–764. https://doi.org/10.4319/lo.1977.22.4.0760.

D'Odorico, P., Okin, G.S., Bestelmeyer, B.T., 2012. A synthetic review of feedbacks and drivers of shrub encroachment in arid grasslands. Ecohydrology 5 (5), 520–530. https://doi.org/10.1002/eco.259.

de Graaff, M.-A., Throop, H.L., Verburg, P.S.J., Arnone, J.A., Campos, X., 2014. A synthesis of climate and vegetation cover effects on biogeochemical cycling in shrub-dominated drylands. Ecosystems 17 (5), 931–945. https://doi.org/10.1007/s10021-014-9764-6.

de Vries, F.T., Griffiths, R.I., Knight, C.G., Nicolitch, O., Williams, A., 2020. Harnessing rhizosphere microbiomes for drought-resilient crop production. Science (80-) 368 (6488), 270–274. https://doi.org/10.1126/science:aaz5192.

Delgado-Baquerizo, M., Guerra, C.A., Cano-Díaz, C., Egidi, E., Wang, J.-T., Eisenhauer, N., Singh, B.K., Maestre, F.T., 2020. The proportion of soil-borne pathogens increases with warming at the global scale. Nat. Clim. Chang. 10 (6), 550–554. https://doi.org/10.1038/s41558-020-0759-3.

Delgado-Baquerizo, M., Maestre, F.T., Eldridge, D.J., Bowker, M.A., Ochoa, V., Gozalo, B., Berdugo, M., Val, J., Singh, B.K., 2016. Biocrust-forming mosses mitigate the negative impacts of increasing aridity on ecosystem multifunctionality in drylands. New Phytol. 209 (4), 1540–1552. https://doi.org/10.1111/nph.13688.

Delgado-Baquerizo, M., Maestre, F.T., Gallardo, A., Bowker, M.A., Wallenstein, M.D., Quero, J.L., Ochoa, V., Gozalo, B., García-Gómez, M., Soliveres, S., García-Palacios, P., Berdugo, M., Valencia, E., Escolar, C., Arredondo, T., Barraza-Zepeda, C., Bran, D., Carreira, J.A., Chaieb, M., Conceição, A.A., Derak, M., Eldridge, D.J., Escudero, A., Espinosa, C.I., Gaitán, J., Gatica, M.G., Gómez-González, S., Guzman, E., Gutiérrez, J.R., Florentino, A., Hepper, E., Hernández, R. M., Huber-Sannwald, E., Jankju, M., Liu, J., Mau, R.L., Miriti, M., Monerris, J., Naseri, K., Noumi, Z., Polo, V., Prina, A., Pucheta, E., Ramírez, E., Ramírez-Collantes, D.A., Romão, R., Tighe, M., Torres, D., Torres-Díaz, C., Ungar, E.D., Val, J., Wamiti, W., Wang, D., Zaady, E., 2013. Decoupling of soil nutrient cycles as a function of aridity in global drylands. Nature 502 (7473), 672–676. https://doi.org/10.1038/nature12670.

Ding, J., Eldridge, D.J., 2020. Biotic and abiotic effects on biocrust cover vary with microsite along an extensive aridity gradient. Plant Soil 450 (1-2), 429–441. https://doi.org/10.1007/s11104-020-04517-0.

Durán, J., Delgado-Baquerizo, M., Dougill, A.J., Guuroh, R.T., Linstädter, A., Thomas, A. D., Maestre, F.T., 2018. Temperature and aridity regulate spatial variability of soil multifunctionality in drylands across the globe. Ecology 99 (5), 1184–1193. https://doi.org/10.1002/ecy.2018.99.issue-510.1002/ecy.2199.

Edgar, R.C., 2016. UNOISE2: improved error-correction for Illumina 16S and ITS amplicon sequencing. bioRxiv 081257. https://doi.org/10.1101/081257v1.

Edgar, R.C., 2010. Search and clustering orders of magnitude faster than BLAST. Bioinformatics 26, 2460–2461. https://doi.org/10.1093/bioinformatics/btq461.

Elliott, D.R., Thomas, A.D., Hoon, S.R., Sen, R., 2014. Niche partitioning of bacterial communities in biological crusts and soils under grasses, shrubs and trees in the Kalahari. Biodivers. Conserv. 23 (7), 1709–1733. https://doi.org/10.1007/s10531-014-0684-8.

Ewing, S.A., Sutter, B., Owen, J., Nishiizumi, K., Sharp, W., Cliff, S.S., Perry, K., Dietrich, W., McKay, C.P., Amundson, R., 2006. A threshold in soil formation at Earth's arid–hyperarid transition. Geochim. Cosmochim. Acta 70 (21), 5293–5322. https://doi.org/10.1016/j.gca.2006.08.020.

Fernández-Alonso, M.J., Curiel Yuste, J., Kitzler, B., Ortiz, C., Rubio, A., 2018. Changes in litter chemistry associated with global change-driven forest succession resulted in time-decoupled responses of soil carbon and nitrogen cycles. Soil Biol. Biochem. 120, 200–211. https://doi.org/10.1016/j.soilbio.2018.02.013.

Fernández-Alonso, M.J., Rodríguez, A., García-Velázquez, L., Dos Santos, E., de Almeida, L., Lafuente, A., Wang, J., Brajesh, S., Fangueiro, D, Durán, J., 2021. Data for: Integrative effects of increasing aridity and biotic cover on soil attributes and functioning in coastal dune ecosystems. Figshare. https://doi.org/10.6084/m9.figshare.12674375.v1.

Fernández, J.A., Niell, F.X., Lucena, J., 1985. A rapid and sensitive automated determination of phosphate in natural waters. Limnol. Oceanogr. 30, 227–230. https://doi.org/10.4319/lo.1985.30.1.0227.

Fick, S.E., Hijmans, R.J., 2017. WorldClim 2: new 1-km spatial resolution climate surfaces for global land areas. Int. J. Climatol. 37 (12), 4302–4315. https://doi.org/10.1002/joc.2017.37.issue-1210.1002/joc.5086.

Fierer, N., Jackson, J.A., Vilgalys, R., Jackson, R.B., 2005. Assessment of soil microbial community structure by use of taxon-specific quantitative PCR assays. Appl. Environ. Microbiol. 71 (7), 4117–4120. https://doi.org/10.1128/AEM.71.7.4117-4120.2005.

Finzi, A.C., Austin, A.T., Cleland, E.E., Frey, S.D., Houlton, B.Z., Wallenstein, M.D., 2011. Responses and feedbacks of coupled biogeochemical cycles to climate change: examples from terrestrial ecosystems. Front. Ecol. Environ. 9 (1), 61–67. https://doi.org/10.1890/100001.

García-Velázquez, L., Rodríguez, A., Gallardo, A., Maestre, F.T., Dos Santos, E., Lafuente, A., Fernández-Alonso, M.J., Singh, B.K., Wang, J., Durán, J., Wang, F., 2020. Climate and soil micro-organisms drive soil phosphorus fractions in coastal dune systems. Funct. Ecol. 34 (8), 1690–1701. https://doi.org/10.1111/fec.v34.810.1111/1365-2435.13606.

Harding, D.E., Ross, D.J., 1964. Some factors in low-temperature storage influencing the mineralisable-nitrogen of soils. J. Sci. Food Agric. 15 (12), 829–834. https://doi.org/10.1002/(ISSN)1097-001010.1002/jsfa.v15:1210.1002/jsfa.2740151203.

Hedley, M.J., Stewart, J.W.B., Chauhan, B.S., 1982. Changes in inorganic and organic soil phosphorus fractions induced by cultivation practices and by laboratory incubations. Soil Sci. Soc. Am. J. 46 (5), 970–976. https://doi.org/10.2136/sssaj1982.03615995004600050017x.

Herlemann, D.P.R., Labrenz, M., Jürgens, K., Bertilsson, S., Waniek, J.J., Andersson, A.F., 2011. Transitions in bacterial communities along the 2000 km salinity gradient of the Baltic Sea. ISME J. 5, 1571–1579. https://doi.org/10.1038/ismej.2011.41.

Herrick, J.E., Zee, J.W. Van, McCord, S.E., Courtright, E.M., Karl, J.W., Burkett, L.M., 2017. Monitoring manual for grassland, shrubland and savanna ecosystems. Volume I: Core Methods. Second Edition. USDA-ARS Jornada Experimental Range, New Mexico, USA.

Hess, H.H., Derr, J.E., 1975. Assay of inorganic and organic phosphorus in the 0.1–5 nanomole range. Anal. Biochem. 63 (2), 607–613. https://doi.org/10.1016/0003-2697(75)90388-7.

Ihrmark, K., Bödeker, I.T.M., Cruz-Martinez, K., Friberg, H., Kubartova, A., Schenck, J., Strid, Y., Stenlid, J., Brandström-Durling, M., Clemmensen, K.E., Lindahl, B.D., 2012. New primers to amplify the fungal ITS2 region - evaluation by 454-sequencing of artificial and natural communities. FEMS Microbiol. Ecol. 82 (3), 666–677. https://doi.org/10.1111/j.1574-6941.2012.01437.x.

IUSS Working Group WRB, 2015. World Reference Base for Soil Resources 2014, update 2015. International soil classification system for naming soils and creating legends for soil maps, World Soil Resources Reports No. 106. FAO, Rome.

Jones, M.L.M., Sowerby, A., Williams, D.L., Jones, R.E., 2008. Factors controlling soil development in sand dunes: Evidence from a coastal dune soil chronosequence. Plant Soil 307 (1-2), 219–234. https://doi.org/10.1007/s11104-008-9601-9.

Lafuente, A., Bowker, M.A., Delgado-Baquerizo, M., Durán, J., Singh, B.K., Maestre, F.T., Xu, X., 2019. Global drivers of methane oxidation and denitrifying gene distribution in drylands. Glob. Ecol. Biogeogr. 28 (9), 1230–1243. https://doi.org/10.1111/geb.v28.910.1111/geb.12928.

Laliberté, E., Turner, B.L., Costes, T., Pearse, S.J., Wyrwoll, K.-H., Zemunik, G., Lambers, H., 2012. Experimental assessment of nutrient limitation along a 2-million-year dune chronosequence in the south-western Australia biodiversity hotspot. J. Ecol. 100, 631–642. https://doi.org/10.1111/j.1365-2745.2012.01962.x.

Lenth, R.V., 2016. Least-squares means: the R package lsmeans. J. Stat. Softw. 69, 1–33. https://doi.org/10.18637/jss.v069.i01.

Li, J., Okin, G.S., Alvarez, L., Epstein, H., 2007. Quantitative effects of vegetation cover on wind erosion and soil nutrient loss in a desert grassland of southern New Mexico, USA. Biogeochemistry 85 (3), 317–332. https://doi.org/10.1007/s10533-007-9142-y.

Linstädter, A., Baumann, G., 2013. Abiotic and biotic recovery pathways of arid rangelands: Lessons from the High Atlas Mountains, Morocco. CATENA 103, 3–15. https://doi.org/10.1016/j.catena.2012.02.002.

Maestre, F.T., Delgado-Baquerizo, M., Jeffries, T.C., Eldridge, D.J., Ochoa, V., Gozalo, B., Quero, José.L., García-Gómez, M., Gallardo, A., Ulrich, W., Bowker, M.A., Arredondo, T., Barraza-Zepeda, C., Bran, D., Florentino, A., Gaitán, J., Gutiérrez, J. R., Huber-Sannwald, E., Jankju, M., Mau, R.L., Miriti, M., Naseri, K., Ospina, A., Stavi, I., Wang, D., Woods, N.N., Yuan, X., Zaady, E., Singh, B.K., 2015. Increasing aridity reduces soil microbial diversity and abundance in global drylands. Proc. Natl. Acad. Sci. U. S. A. 112 (51), 15684–15689. https://doi.org/10.1073/pnas.1516684112.

Maestre, F.T., Quero, J.L., Gotelli, N.J., Escudero, A., Ochoa, V., Delgado-Baquerizo, M., Garcia-Gomez, M., Bowker, M.A., Soliveres, S., Escolar, C., Garcia-Palacios, P., Berdugo, M., Valencia, E., Gozalo, B., Gallardo, A., Aguilera, L., Arredondo, T., Blones, J., Boeken, B., Bran, D., Conceicao, A.A., Cabrera, O., Chaieb, M., Derak, M., Eldridge, D.J., Espinosa, C.I., Florentino, A., Gaitan, J., Gatica, M.G., Ghiloufi, W., Gomez-Gonzalez, S., Gutierrez, J.R., Hernandez, R.M., Huang, X., Huber-Sannwald, E., Jankju, M., Miriti, M., Monerris, J., Mau, R.L., Morici, E., Naseri, K., Ospina, A., Polo, V., Prina, A., Pucheta, E., Ramirez-Collantes, D.A., Romao, R., Tighe, M., Torres-Diaz, C., Val, J., Veiga, J.P., Wang, D., Zaady, E., 2012. Plant species richness and ecosystem multifunctionality in global drylands. Science (80-). 335, 214–218. https://doi.org/10.1126/science.1215442.

Mikkonen, N., Moilanen, A., 2013. Identification of top priority areas and management landscapes from a national Natura 2000 network. Environ. Sci. Policy 27, 11–20. https://doi.org/10.1016/j.envsci.2012.10.022.

Mo, Y., Kearney, M.S., Turner, R.E., 2020. The resilience of coastal marshes to hurricanes: The potential impact of excess nutrients. Environ. Int. 138, 105409. https://doi.org/10.1016/j.envint.2019.105409.

Nelson, D.W., Sommers, L.E., 1996. Total carbon, organic carbon, and organic matter, in: Sparks, D., Page, A., Helmke, P., Loeppert, R., Soltanpour, P.N., Tabatabai, M.A., Johnston, C.T., Sumner, M.E. (Eds.), Methods of Soil Analysis. Part 3. Chemical Methods. SSSA Book Series no 5, Madison, USA., pp. 961–1010. https://doi.org/10.2136/sssabookser5.3.c34.

Ochoa-Hueso, R., Eldridge, D.J., Delgado-Baquerizo, M., Soliveres, S., Bowker, M.A., Gross, N., Le Bagousse-Pinguet, Y., Quero, J.L., García-Gómez, M., Valencia, E., Arredondo, T., Beinticinco, L., Bran, D., Cea, A., Coaguila, D., Dougill, A.J., Espinosa, C.I., Gaitán, J., Guuroh, R.T., Guzman, E., Gutiérrez, J.R., Hernández, R. M., Huber-Sannwald, E., Jeffries, T., Linstädter, A., Mau, R.L., Monerris, J., Prina, A., Pucheta, E., Stavi, I., Thomas, A.D., Zaady, E., Singh, B.K., Maestre, F.T., Salguero-Gómez, R., 2018. Soil fungal abundance and plant functional traits drive fertile island formation in global drylands. J. Ecol. 106 (1), 242–253. https://doi.org/10.1111/jec.2018.106.issue-110.1111/1365-2745.12871.

Okin, G.S., Heras, M.-de las., Saco, P.M., Throop, H.L., Vivoni, E.R., Parsons, A.J., Wainwright, J., Peters, D.PC., 2015. Connectivity in dryland landscapes: shifting concepts of spatial interactions. Front. Ecol. Environ. 13 (1), 20–27. https://doi.org/10.1890/140163.

Pansu, M., Gautheyrou, J., 2006. Handbook of Soil Analysis. Mineralogical, Organic and Inorganic Methods. Springer-Verlag, Berlin, Heidelberg. https://doi.org/10.1007/978-3-540-31211-6.

Pausas, J.G., Austin, M.P., 2001. Patterns of plant species richness in relation to different environments: an appraisal. J. Veg. Sci. 12 (2), 153–166. https://doi.org/10.2307/3236601.

Pinheiro, J., Bates, D., DebRoy, S., Sarkar, D., R Core Team, 2017. nlme: Linear and nonlinear mixed effects models.

Plaza, C., Zaccone, C., Sawicka, K., Méndez, A.M., Tarquis, A., Gascó, G., Heuvelink, G.B. M., Schuur, E.A.G., Maestre, F.T., 2018. Soil resources and element stocks in drylands to face global issues. Sci. Rep. 8, 13788. https://doi.org/10.1038/s41598-018-32229-0.

Pumpanen, J., Kolari, P., Ilvesniemi, H., Minkkinen, K., Vesala, T., Niinistö, S., Lohila, A., Larmola, T., Morero, M., Pihlatie, M., Janssens, I., Yuste, J.C., Grünzweig, J.M., Reth, S., Subke, J.-A., Savage, K., Kutsch, W., Østreng, G., Ziegler, W., Anthoni, P., Lindroth, A., Hari, P., 2004. Comparison of different chamber techniques for measuring soil CO_2 efflux. Agric. For. Meteorol. 123 (3-4), 159–176. https://doi.org/10.1016/j.agrformet.2003.12.001.

R Core Team, 2019. R: A language and environment for statistical computing.

Rodríguez, A., Curiel Yuste, J., Rey, A., Durán, J., García-Camacho, R., Gallardo, A., Valladares, F., 2017. Holm oak decline triggers changes in plant succession and microbial communities, with implications for ecosystem C and N cycling. Plant Soil 414 (1-2), 247–263. https://doi.org/10.1007/s11104-016-3118-4.

Rodríguez, A., Durán, J., Fernández-Palacios, J.M., Gallardo, A., 2009. Short-term wildfire effects on the spatial pattern and scale of labile organic-N and inorganic-N and P pools. For. Ecol. Manage. 257 (2), 739–746. https://doi.org/10.1016/j.foreco.2008.10.006.

Rodríguez, A., Durán, J., Rey, A., Boudouris, I., Valladares, F., Gallardo, A., Yuste, J.C., 2019. Interactive effects of forest die-off and drying-rewetting cycles on C and N mineralization. Geoderma 333, 81–89. https://doi.org/10.1016/j.geoderma.2018.07.003.

Schimel, J.P., Bennett, J., 2004. Nitrogen mineralization: challenges of a changing paradigm. Ecology 85 (3), 591–602. https://doi.org/10.1890/03-8002.

Sevink, J., 1991. Soil development in the coastal dunes and its relation to climate. Landsc. Ecol. 6 (1-2), 49–56. https://doi.org/10.1007/BF00157744.

Sims, G.K., Ellsworth, T.R., Mulvaney, R.L., 1995. Microscale determination of inorganic nitrogen in water and soil extracts. Commun. Soil Sci. Plant Anal. 26 (1-2), 303–316. https://doi.org/10.1080/00103629509369298.

Tiessen, H., Moir, J.O., 2006. Characterization of available p by sequential extraction. In: Carter, M.R., Gregorich, E.G. (Eds.), Soil Sampling and Methods of Analysis. CRC Press, Boca Raton, USA, pp. 293–306 https://doi.org/https://doi.org/10.1201/9781420005271.

Trabucco, A., Zomer, R., 2019. Global Aridity Index and Potential Evapotranspiration (ET0) Climate Database v2.figshare. Fileset.

Ulrich, W., Soliveres, S., Maestre, F.T., Gotelli, N.J., Quero, J.L., Delgado-Baquerizo, M., Bowker, M.A., Eldridge, D.J., Ochoa, V., Gozalo, B., Valencia, E., Berdugo, M., Escolar, C., García-Gómez, M., Escudero, A., Prina, A., Alfonso, G., Arredondo, T., Bran, D., Cabrera, O., Cea, A.P., Chaieb, M., Contreras, J., Derak, M., Espinosa, C.I., Florentino, A., Gaitán, J., Muro, V.G., Ghiloufi, W., Gómez-González, S., Gutiérrez, J. R., Hernández, R.M., Huber-Sannwald, E., Jankju, M., Mau, R.L., Hughes, F.M., Miriti, M., Monerris, J., Muchane, M., Naseri, K., Pucheta, E., Ramírez-Collantes, D. A., Raveh, E., Romão, R.L., Torres-Díaz, C., Val, J., Veiga, J.P., Wang, D., Yuan, X., Zaady, E., Daniel Kissling, W., 2014. Climate and soil attributes determine plant species turnover in global drylands. J. Biogeogr. 41 (12), 2307–2319. https://doi.org/10.1111/jbi.12377.

Wang, X.-G., Lü, X.-T., Zhang, H.-Y., Dijkstra, F.A., Jiang, Y.-G., Wang, X.-B., Lu, J.-Y., Wuyunna, Wang, Z.-W., Han, X.-G., 2020. Changes in soil C:N: P stoichiometry along an aridity gradient in drylands of northern China. Geoderma 361, 114087. https://doi.org/10.1016/j.geoderma.2019.114087.

Wei, T., Simko, V., 2017. R package “corrplot”: Visualization of a Correlation Matrix (Version 0.84).

Yuan, Z., Gazol, A., Wang, X., Xing, D., Lin, F., Bai, X., Zhao, Y., Li, B., Hao, Z., 2012. What happens below the canopy? Direct and indirect influences of the dominant species on forest vertical layers. Oikos 121 (7), 1145–1153. https://doi.org/10.1111/more.2012.121.issue-710.1111/j.1600-0706.2011.19757.x.

Zuo, X.A., Zhao, X.Y., Zhao, H.L., Guo, Y.R., Zhang, T.H., Cui, J.Y., 2010. Spatial pattern and heterogeneity of soil organic carbon and nitrogen in sand dunes related to vegetation change and geomorphic position in Horqin Sandy Land, Northern China. Environ. Monit. Assess. 164 (1-4), 29–42. https://doi.org/10.1007/s10661-009-0872-2.